ELSEVIER

Remote Sensing of Environment 77 (2001) 367–376

Remote Sensing of Environment

www.elsevier.com/locate/rse

Radiometric characterization of field radiometers in support of the 1997 Lunar Lake, Nevada, experiment to determine surface reflectance and top-of-atmosphere radiance

Steven W. Brown[a,*], B. Carol Johnson[a], Howard W. Yoon[a], James J. Butler[b], Robert A. Barnes[c], Stuart Biggar[d], Paul Spyak[d,1], Kurtis Thome[d], Edward Zalewski[d], Mark Helmlinger[e], Carol Bruegge[e], Stephen Schiller[f], Gunar Fedosejevs[g], Robert Gauthier[g], Satoshi Tsuchida[h], Shoichi Machida[i]

[a]*National Institute of Standards and Technology, 100 Bureau Drive, Stop 8442, Gaithersburg, MD 20899-844, USA*
[b]*NASA's Goddard Space Flight Center, Greenbelt, MD, USA*
[c]*SAIC/General Sciences Corporation, Laurel, MD, USA*
[d]*University of Arizona, Tucson, AZ, USA*
[e]*NASA's Jet Propulsion Laboratory, California Institute of Technology, Pasadena, CA, USA*
[f]*South Dakota State University, Brookings, SD, USA*
[g]*Canadian Center for Remote Sensing, Ottawa, Canada*
[h]*Geological Survey of Japan, Tsukuba, Japan*
[i]*Earth Remote Sensing Data Analysis Center, Tokyo, Japan*

Abstract

A continuing series of field campaigns to Lunar Lake, Nevada, has been established to develop measurement protocols and assess the uncertainties of ground-based calibrations of on-orbit satellite sensors. In June 1997, an ensemble of field radiometers was deployed to validate the fundamental reflectance and radiance measurements of the Land Satellite (Landsat-5) Thematic Mapper (TM) and Satellite Pour l'Observation de la Terre (SPOT-2) Haute Resolution Visible (HRV) satellite instruments. Prior their deployment to Lunar Lake, many of the field instruments measured a common sphere source at the University of Arizona (UA). The results, presented in this work, showed variations in the relative stabilities of the field instruments, and demonstrate the need for in-depth characterization of field instruments for an accurate assessment of instrument performance and measurement uncertainty. © 2001 Published by Elsevier Science Inc.

1. Introduction

The development of ground-truth measurements for the on-orbit calibration of satellite sensors, also known as vicarious calibration, has produced a number of continuing field campaigns at target sites all over the world. One example is the annual field campaign to Lunar Lake, Nevada, in which international remote sensing research groups measure the surface reflectance of the playa from the air and the ground during periods of satellite overflights (Slater, Biggar, Thome, Gellman, & Spyak, 1996; Thome, Schiller, Conel, Arai, & Tsuchida, 1998). During the field measurements, the signal from a small area of the playa is measured followed by a measurement of a calibrated reflectance panel. This sequence is repeated until a set area of the playa, determined from the instantaneous field-of-view (IFOV) of the satellite sensor to be calibrated, has been measured. The reflectance panel data are subsequently used to normalize the playa data to obtain an average playa reflectance over the measurement area. These measurements, along with a measurement of the solar atmospheric transmittance and selection of an exoatmospheric solar irradiance model, are then input into a radiative transfer model to calculate the predicted top-of-atmosphere (TOA) radiance measured by the satellite sensor (Slater et al., 1996; Thome et al., 1998).

Typically, research groups with varied instrumentation and measurement techniques participate in the field cam-

* Corresponding author. Tel.: +1-301-975-5167.
E-mail address: steven.brown@nist.gov (S.W. Brown).
[1] Current address: Raytheon Systems, Tucson, AZ, USA.

PII: S0034-4257(01)00215-2

paigns. The 1996 Lunar Lake campaign was primarily designed to compare TOA radiances as determined by the participants, and no satellite sensor overpasses occurred during the campaign. Results from the 1996 field campaign showed differences in predicted TOA radiances between the groups ranging from 5% to 15% over the spectral range from 400 to 2500 nm (Thome et al., 1998). The 1996 campaign identified several sources contributing to the overall measurement uncertainty. These sources included errors in the reference target reflectance values, instabilities in the responsivities of the field instruments, and differences in solar irradiance spectra and radiative transfer codes used in the calculation of the TOA radiance.

The 1997 Lunar Lake campaign was designed to examine these sources of uncertainty and to compare TOA radiances predicted by the campaign participants with radiances measured by the overpassing the Satellite Pour l'Observation de la Terre (SPOT-2) Haute Resolution Visible (HRV) and Land Satellite (Landsat-5) Thematic Mapper (TM) satellite sensors. In order to examine the contributions of the error sources to the overall measurement uncertainty, the 1997 campaign featured two pre-field-campaign experiments, held at the University of Arizona (UA) Optical Sciences Center. In these laboratory measurements, differences in the reference target reflectance values and instabilities in the responsivities of the field instruments were examined. The first experiment involved measuring the bidirectional reflectance distribution function (BRDF) of reference targets used in the field against a National Institute of Standards and Technology (NIST) standard reference target. Several panels were again measured at UA following the field campaign to verify that the panel reflectances had not changed.

In the second experiment, the campaign field radiometers measured a common, stable, uniform, integrating sphere source to assess the short-term stability of the instruments. In addition, the linearity of the response of two of the instruments was measured and the radiance calibration of one instrument was examined. This paper presents the results of a laboratory assessment of the performance of the field radiometers. In Section 2, a brief description of the instrumentation used in the experiment is given. In Section 3, the experimental procedures are outlined. Results are presented and discussed in Section 4 and summarized in Section 5.

2. Instrumentation

Three types of instrumentation were used during the intercomparison: an integrating sphere source, calibrated transfer radiometers, and field instruments. The sphere source should ideally be a uniform, stable, Lambertian source giving signals similar to those measured during the field campaign over the entire wavelength range of interest, namely 400–2500 nm. The transfer radiometers are stable, well-characterized instruments used to measure the absolute radiance of the integrating sphere source. During the intercomparison, the transfer radiometers were also used to monitor the sphere stability. The field instruments are designed for measurements in remote environments. They are typically lightweight, self-contained units, and are often battery-powered. The integrating sphere source, the transfer radiometers, and the field instruments used in the UA measurement intercomparison are briefly described below.

2.1. Integrating sphere source

A Labsphere[2] Model USS-4000 Integrating Sphere was used as a stable, uniform radiance source for the measurements. It is a 100-cm diameter sphere, coated with barium sulfate, with a 35-cm diameter exit aperture. The integrating sphere source is configured with a total of 15 incandescent lamps: ten 150-W lamps, three 45-W lamps, one 30-W lamp, and one 6-W lamp. The sphere source was run in three configurations: high-level radiance, using ten 150-W lamps; medium-level radiance, using three 150 W-lamps; and low-level radiance, using one 45-W lamp and one 30-W lamp. A silicon (Si) photodiode with a photopic filter (i.e., with a visible bandpass) was mounted on the sphere to monitor the relative radiance output. The photodiode was not temperature stabilized.

2.2. Transfer radiometers

A total of three stable, well-characterized, filter-based radiometers were used to measure and to monitor the sphere radiance: the Earth Observing System (EOS) Visible Transfer Radiometer (VXR), the UA Visible/Near-Infrared Radiometer (UA VNIR), and the UA Short-Wave Infrared Radiometer (UA SWIR).

The VXR was designed and built by NIST for the EOS Project Science Office at NASA's Goddard Space Flight Center. The VXR is an improved version of the Sea-Viewing, Wide Field-of-View Sensor Transfer Radiometer (Johnson, Fowler, & Cromer, 1998). Both instruments use a camera lens to focus the object at the field stop. Behind the field stop, six wedge-shaped mirrors with spherical curvature focus the field stop at six image locations, where individual interference filters and Si photodiodes are located. The temperature of the field stop, filters, and detectors is maintained at 26°C. An on-axis optical system is used to align and focus the VXR. The field-of-view (FOV) of the VXR is 2.5° and the minimum object distance is 85 cm. The band center wavelengths, bandpasses, and relative combined standard uncertainties for the six VXR channels are given in Table 1.

[2] Identification of commercial equipment does not imply recommendation or endorsement by the NIST, nor does it imply that the equipment identified is necessarily the best available for the purpose.

Table 1
Measurement wavelengths, spectral bandwidths, and combined standard uncertainties ($k=1$) of radiance measurements with the VXR transfer radiometer

Channel	Wavelength (nm)	Bandwidth (nm)	Uncertainty (%)
1	411.43	10.8	2.0
2	441.62	10.3	2.0
3	547.96	10.4	2.0
4	661.82	9.6	2.0
5	774.78	11.6	2.0
6	870.0	12	3.0

The UA VNIR is an eight-channel filter radiometer with a detector employing three Si photodiodes (p-on-n type) arranged in a light trapping configuration (Biggar, 1998; Biggar & Slater, 1993). It was built and independently characterized by the UA Optical Sciences Center Remote Sensing Group. Seven narrow-band interference filters are used for spectral selection with the eighth filter position shuttered to enable measurement of the radiometer dark signal. To enhance stability, the temperature of the filters and detectors is maintained at 30°C. Two precision apertures are separated by a precisely measured distance fix the FOV and throughput of the radiometer. Band center wavelengths, spectral bandpasses, and relative combined standard uncertainties are given in Table 2.

The UA SWIR is a nine-channel filter radiometer incorporating an indium antimonide (InSb) photodiode as its detector. Light incident on the radiometer is chopped, and the detector output is sent to a lock-in amplifier. As with the UA VNIR, a pair of precision apertures separated by a known distance determines the SWIR radiometer's FOV. To reduce noise and increase sensitivity, the InSb detector is operated at liquid nitrogen temperature (77 K). To further reduce unwanted thermal infrared background signal, a cold filter within the Dewar assembly is used to block radiation at wavelengths longer than 2.7 μm. Nine narrow band interference filters are used for spectral selection; their band centers and bandpasses are listed in Table 3.

2.3. Field instrumentation

A total of 11 instruments participated in the intercomparison. The results from eight instruments, described below, are presented in this work.

Table 2
Measurement wavelengths, spectral bandwidths, and combined standard uncertainties ($k=1$) of radiance measurements with the UA VNIR transfer radiometer

Channel	Wavelength (nm)	Bandwidth (nm)	Uncertainty (%)
1	412.8	15.1	2.2
2	441.8	11.9	2.2
3	488.0	9.7	2.2
4	550.3	9.9	2.2
5	666.5	9.8	2.2
6	746.9	10.7	2.2
7	868.1	14.0	2.2

Two types of instruments from Analytical Spectral Devices participated in the measurement intercomparison. Both instruments are portable spectroradiometers employing hand-held input optics coupled to the spectrometer through a fiber bundle. The first instrument, a Personal Spectrometer II (PSII), is a fixed grating, Si diode array system with a spectral range from 350 to 1100 nm and a nominal resolution of 3 nm. The second instrument, a FieldSpec FR portable spectroradiometer, has three grating spectrometers and associated detectors enabling measurements to be made over a wavelength range from 350 to 2500 nm. The first spectrometer uses a 512 element, Si photodiode array with a fixed grating, and is designed for the wavelength range from 350 to 1050 nm. The second spectrometer, designed for the wavelength range from 900 to 1850 nm, uses a scanned grating and a single element, thermoelectrically cooled indium gallium arsenide (InGaAs) detector. The final spectrometer element also uses a scanned grating configuration with a thermoelectrically cooled InGaAs detector for the wavelength range from 1700 to 2500 nm. The instrument has a spectral resolution of approximately 3 nm at 700 nm, 10 nm at 1500 nm, and 10 nm at 2100 nm. Fore-optics with FOVs of 1°, 3°, 5°, 8°, 18°, and 24° are available.

Two spectroradiometers from the Geophysical and Environmental Research Corporation (GER) participated in the measurement intercomparison, a GER Mark V Infra-Red Intelligent Spectroradiometer (IRIS) and a GER 3700. The Mark V is a scanned grating instrument with a wavelength range from 350 to 2500 nm. It utilizes two thermoelectrically cooled detectors: Si for the wavelength range from 300 to 1000 nm and lead sulfide (PbS) for the 1000- to 2500-nm range. Order-sorting filters eliminate second-order diffraction effects. The spectral resolution is approximately 4 nm in the visible to near-infrared (350–1000 nm) and 10 nm in the short-wave infrared (1050–2500 nm). The incident radiation is chopped; the output from the detector is measured using phase-sensitive detection. The Mark V instrument comes equipped with interchangeable fore-optics with FOVs of 3° and 7°. The GER 3700 Series spectroradiometer is an array-based system operating over the wavelength range from 350 to 2500 nm. It is comprised of three separate spectroradiometers, utilizing one 512 element Si array for

Table 3
Measurement wavelengths, spectral bandwidths, and combined standard uncertainties ($k=1$) of radiance measurements with the UA SWIR transfer radiometer

Filter	Wavelength (nm)	Bandwidth (nm)	Uncertainty (%)
1	1243.5	15.2	3.3
2	1380.8	29.0	uncalibrated
3	1646.0	23.4	3.3
4	2133.6	55.1	3.6
5	2164.3	40.8	3.6
6	2207.9	44.5	3.7
7	2263.0	49.3	3.7
8	2332.3	63.1	3.8
9	2403.2	70.3	3.9

Table 4
PARABOLA bands, center wavelengths, and bandwidths

Band	Center wavelength (nm)	Bandwidth (nm)
1	440	32
2	550	27
3	650	29
4	1030	22
PAR	550	319
6	860	33
7	940	22
8	1665	70

the wavelength range from 350 to 1150 nm, one 128 element PbS array for the wavelength range from 1150 to 1800 nm, and one 64 element PbS array for the range from 1800 to 2500 nm. The nominal bandpass of the instrument is 2.5 nm for the Si array, 7–14 nm for the 128 element PbS array, and 12–16 nm for the 64 element, PbS array. The array detectors are not temperature-stabilized. The FOV of the entrance aperture optics was 10°.

The Portable Apparatus for Rapid Acquisition of Bidirectional Observation of the Land and Atmosphere III (PARABOLA) is a field radiometer built by Sensit of North Dakota and operated by NASA's Jet Propulsion Laboratory (JPL). It is a sphere-scanning, multispectral radiometer system that generates radiance measurements for both the downward and upward looking hemispheres by sampling the sphere at 2664 view angles (Deering & Leone, 1986). PARABOLA consists of three elements: a sensor head mounted on a motor-driven two-axis gimbal, a data recording and control unit, and a power pack. The system employs thermoelectrically cooled Si and germanium detectors for the visible and NIR bands. Filter and bandwidth specifications are listed in Table 4.

The optical head of PARABOLA consists of two banks of detectors and filters with 2° FOV tubes each with three channels (expandable to four) mounted along a horizontal axis at opposite ends of a cylindrical housing. During the sphere measurements, the PARABOLA head remained stationary while one of the detector banks acquired data. The arm was then rotated 180° and a set of data was taken with the second bank of detectors. The instrument was aligned such that both sets of detectors measured the radiance from the central portion of the sphere.

3. Experimental

Integrating sphere measurements were made over the course of 4 days, from 17 June 1997 to 20 June 1997. The three transfer radiometers measured the sphere radiance at the beginning and at the end of each measurement sequence to assess the sphere stability over the course of the measurements. Similarly, during measurements using field instruments, one of the standard transfer radiometers was aligned to measure the sphere output continuously off-axis. On the 17th and 18th of June, the VXR was set up 30° off-axis to continuously monitor the sphere output at all six channels during field radiometer measurements. On subsequent days, the UA SWIR monitored the sphere radiance at 1646 nm at a direction 36° off-axis to the sphere.

On June 17, a short series of measurements was performed at the high radiance level. In particular, the UA FieldSpec FR took data continuously for 50 min, providing information about the short-term stability of the instrument.

On June 18, both medium- and high-level sphere measurements were made. The FieldSpec FR has a collection head coupled to the spectroradiometer via a fiber optic cable. This collection head was rotated about the viewing axis, with data sets taken every 90°, to look for orientation effects in the radiance measurements. In a second stability test, the FieldSpec FR measured the sphere radiance before and after removing the fiber optic cable from the collection head. Finally, many of the field instruments measured the sphere radiance twice approximately an hour apart to check the reproducibility of the instrumentation. High-level radiance measurements were subsequently made to test the linearity of the instrumentation.

Medium-level sphere measurements were repeated on the 19th, with instruments turned on an hour or more before making any measurements. On the 20th, low-level radiance measurements were made to test the linearity of the field radiometers.

4. Results and discussion

In this section, the stability of the integrating sphere source is discussed, and the reproducibility, linearity, and absolute radiance calibration results of the field instruments are presented.

4.1. Stability of the integrating sphere source

The sphere radiance values measured by the VXR and the UA SWIR at the three operating levels are given in Table 5. All stability measurements of the field instruments were made in the medium-level radiance configuration. The spectral radiance of the integrating sphere, measured by the South Dakota State University (SDSU) FieldSpec FR instrument, is shown in Fig. 1 for the medium-level sphere setting.

Over the course of the day, the sphere radiance, as measured by the Si monitor photodiode, decreased on the order of 0.5%. For example, in Fig. 2 we show monitor data from the 18th of June. On this day, the monitor photodiode signal decreased a total of approximately 0.5% over the course of 7 h, beginning 1 h after the sphere was turned on. The transfer radiometers recorded a similar trend. In Fig. 3, the difference in measured sphere radiance for the VXR and the UA VNIR between the beginning and the end of the day is shown. The sphere radiance has changed approximately

Table 5
Sphere radiance measured by the VXR (411.5–870.0 nm) and the UA SWIR (1243.5–2403.2 nm)

Wavelength (nm)	High-level radiance ($\mu W/cm^2/nm/sr$)	Medium-level radiance ($\mu W/cm^2/nm/sr$)	Low-level radiance ($\mu W/cm^2/nm/sr$)
411.53	11.87	3.51	0.56
441.62	19.27	5.67	0.89
547.96	60.04	17.72	2.67
661.82	105.79	31.25	4.59
774.78	134.59	39.88	5.74
870.0	143.24	42.46	6.01
1243.5		29.35	4.04
1380.8		20.71	2.85
1646.0		12.08	1.62
2133.6		3.15	0.413
2164.3		3.18	0.418
2207.9		3.14	0.412
2263.0		2.77	0.363
2332.3		1.90	0.248
2403.2		1.59	0.207

0.7% at 411 nm and 0.3% at 870 nm. Also shown are VXR data corrected for the change in the Si monitor diode signal. The monitor photodiode underestimates the change in the sphere radiance below 600 nm and overestimates the change in the radiance beyond 700 nm. This is in agreement with expectations, as sphere sources typically change more in the blue spectral region than in the red.

On June 19 and 20, the UA SWIR monitored the sphere radiance at 1646 nm. The sphere radiance changed on the order of 0.1% over the course of several hours on both days. The UA SWIR measurements taken at the beginning and the end of the day on June 19 and 20 recorded a similar trend, with the measured sphere radiance changing by 0.33% or less for all channels with the exception of the 1380.8 nm water absorption band. In Table 6, the total change in sphere radiance measured with the VXR and the UA SWIR from the beginning to the end of the measurements for each day and each lamp setting is shown. The total change in sphere radiance was less than 1% at all wavelengths.

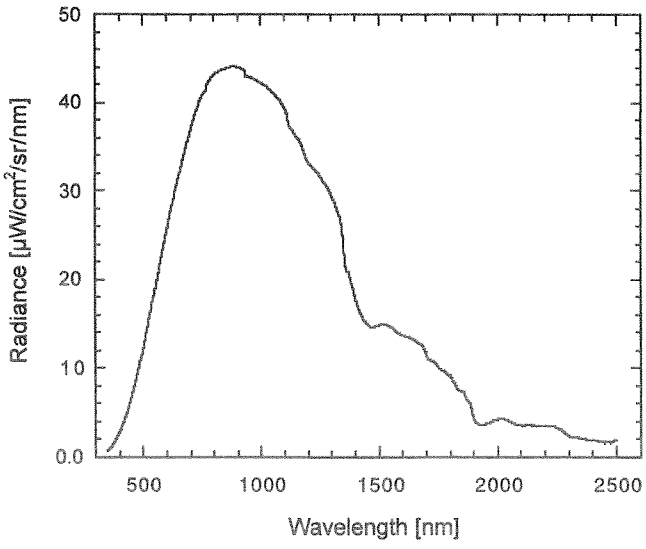

Fig. 1. Medium-level (three-lamp) integrating sphere source radiance measured by the SDSU FieldSpec FR spectroradiometer.

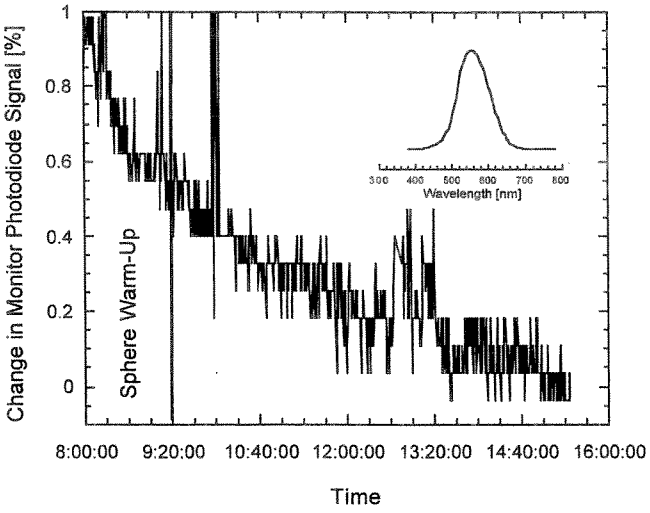

Fig. 2. Relative change in the output of the Si monitor photodiode on the 18th of June. The sphere radiance was set to the medium level. Inset: Relative spectral response of the Si monitor diode with a photopic filter.

4.2. Stability and repeatability of the field instrumentation

Two PSIIs, the SDSU PSII and the GSJ PSII, measured the radiance of the integrating sphere source on the 18th of June. The SDSU PSII was equipped with a 1° FOV fore-optic whereas the GSJ PSII used an 18° FOV fore-optic. Each instrument measured the sphere twice, with approximately 1 h between measurements. Ten scans were averaged for each measurement. Results of these measurements

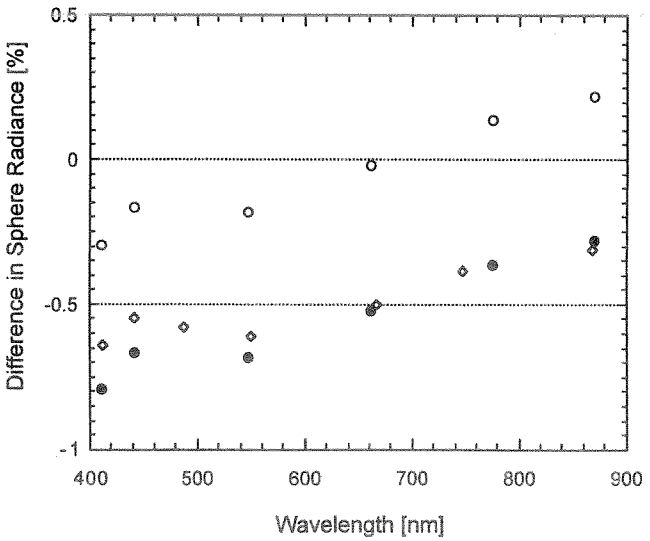

Fig. 3. Difference in sphere radiance measured by the VXR (closed circles) and the UA VNIR (diamonds) between the beginning and the end of measurements on June 18 (approximately 7 h elapsed time). Open circles represent VXR data corrected for the relative change in the Si monitor photodiode signal over the course of the day.

Table 6
The total percent decrease in sphere radiance measured by the VXR (411.5–870.0 nm) and the UA SWIR (1243.5–2403.2 nm) between the beginning and the end of a measurement sequence for a particular lamp setting

Wavelength (nm)	17 June (10–150 W)	18 June (3–150 W)	18 June (10–150 W)	19 June (3–150 W)	20 June (1–45 and 1–30 W)
411.53	0.24	0.80	0.50	0.94	0.35
441.62	0.24	0.67	0.40	0.81	0.26
547.96	0.57	0.69	0.38	0.72	0.16
661.82	0.52	0.52	0.25	0.56	0.10
774.78	0.50	0.37	0.24	0.45	0.09
870.00	0.38	0.28	0.21	0.39	0.11
1243.5				0.23	0.20
1380.8				0.81	0.08
1646.0				0.11	0.11
2133.6				0.13	0.10
2164.3				0.23	0.11
2207.9				0.26	0.14
2263.0				0.33	0.23
2332.3				0.24	0.11
2403.2				0.33	0.08

are shown in Fig. 4. As shown in Fig. 4(a), the SDSU PSII measured a difference as large as 8% around 400 nm, decreasing to roughly 2% at 900 nm. The sphere monitor diode data show that the large differences observed with the SDSU instrument cannot be attributed to changes in the sphere radiance. The standard deviation of the mean of the 10 individual scans acquired by the SDSU PSII for the second measurement is shown in Fig. 4(c). These data are typical of the standard deviations of data acquired with PSII instruments. The standard deviations of the means of the individual scans (Fig. 4(c)) imply that the results cannot be attributed to short-term instabilities in the instrument.

The GSJ PSII, on the other hand, measured a very small difference in sphere radiance, less than 0.5%, over the range from 450 to 950 nm (Fig. 4(b)). The different results obtained by the two PSII instruments remain unexplained, and illustrate the need for further work to fully characterize the short-term stability and repeatability of these instruments.

A total of three FieldSpec FR instruments operated by the UA, SDSU, and JPL measured the sphere. The UA instrument had a FOV of 5°; the SDSU and the JPL instrument had FOVs of 8°.

To assess the short-term stability of the instrument, the UA FieldSpec FR measured the sphere radiance continuously for approximately 50 min on the 17th of June. The sphere was operated in the high-radiance level for these measurements. In Fig. 5, the differences in sphere radiance are shown for total elapsed times between measurements of 5, 25, and 45 min. In the spectral region below 500 nm, the measured sphere radiance decreased greater than 2% at 350 nm after 5 min, and greater than 2% at 400 nm after 25 min. In the region from 500 to 1000 nm, the measured radiance increased continuously with time, with the magnitude of the change increasing with increasing wavelength. The maximum difference was approximately 1.7% at 1000 nm after 45 min. In the region from 1100 to 1700 nm, the measured radiance fluctuated about a mean difference of −0.2%, with the exception of the water-absorption region around 1380 nm. Differences greater than 2% were observed in the

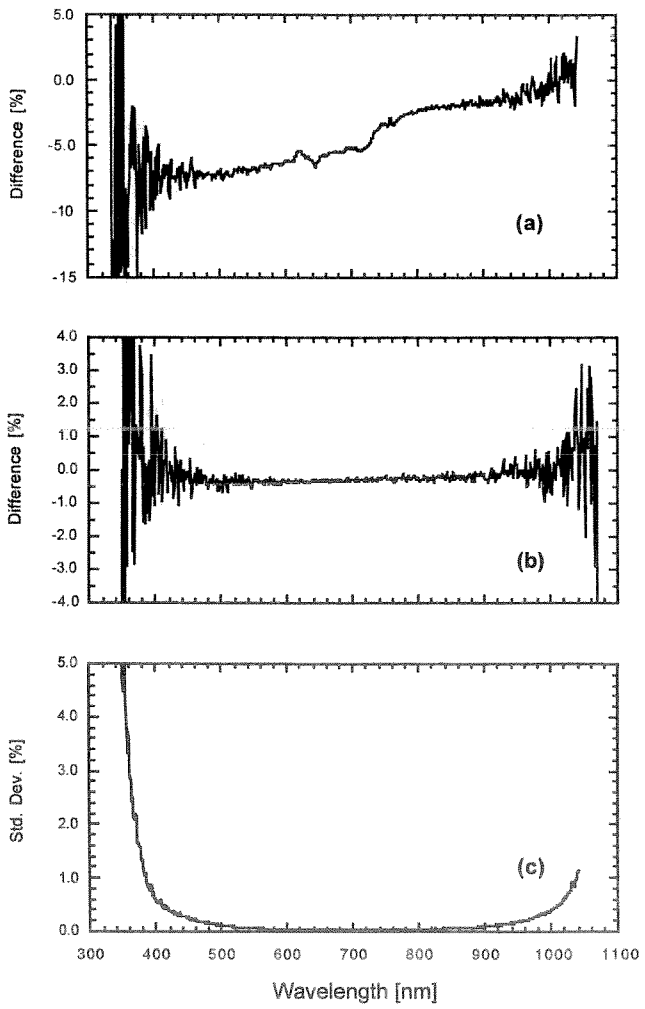

Fig. 4. Difference in sphere radiance measured by (a) the SDSU PSII and (b) the GSJ PSII 1 h apart. (c) The standard deviation of the mean of 10 scans averaged for one SDSU PSII sphere radiance measurement.

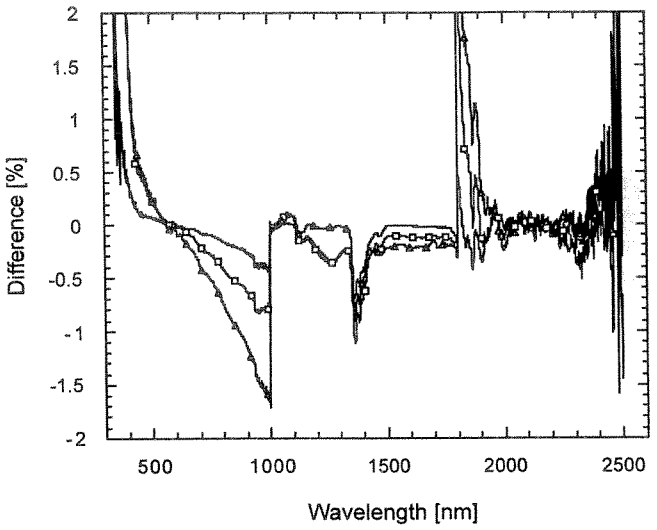

Fig. 5. Difference in sphere radiance measurements using the UA FieldSpec FR. The total elapsed time between measurements was 5 min (solid line), 25 min (open squares), and 45 min (open triangles).

wavelength region from 1800 to 2000 nm and again at approximately 2500 nm.

The sphere radiance, as measured by the monitor photodiode, changed on the order of 0.1% over this time frame. The observed differences are therefore attributed to temporal changes in instrument responsivity.

All three FieldSpec FR spectroradiometers measured the sphere twice on both June 18 and 19, with the time between measurements fixed at approximately 1 h. On the 18th of June, no attention was paid to the time the instruments were turned on prior to measuring the sphere. On the 19th of June, the UA and the SDSU FieldSpec FR instruments were turned on approximately 1 h prior to measuring the sphere while the JPL FieldSpec FR was turned on shortly before making measurements. Results of the measurements are shown in Fig. 6.

The UA instrument showed the largest variation in repeatability between the 2 days (Fig. 6(a)). The UA measurements taken on the 18th of June show differences ranging from 1% to 5% in the 450- to 1000-nm range, and from 0.5% to 2% in the 1000- to 1700-nm range. On June 19, when the instrument was turned on for an hour prior to use, the measurements agreed to within 1%, with the exception of the wavelength regions below 450 nm and above 2400 nm. These data imply that turning the instrument on an hour prior to use significantly improved the repeatability of the measurements.

Measurements taken on both days with the SDSU instrument (Fig. 6(b)) and the JPL instrument (Fig. 6(c)) agreed to within 1% over the spectral ranges from 500 to 900 nm, 1050 to 1750 nm, and 2000 to 2400 nm. For both instruments, changes as large as 3% were observed in the 900- to 1000-nm range. These changes are attributed to differences in the thermal environments of the Si array detectors.

To assess the reproducibility of the SDSU FieldSpec FR, sphere measurements on the 18th and 19th of June were compared. The difference between the mean radiance measured on the 2 days agreed within the combined uncertainties of the repeatability of the measurements on each individual day. Also, configuration effects did not noticeably affect the sphere radiance measurements. Differences in measured sphere radiance when the UA FieldSpec FR was rotated about its axis and when the fiber bundle was removed and reinserted into the fore-optic were within the repeatability of the measurements.

Two sets of measurements were made with the GER Mark V IRIS approximately 15 min apart. Results are shown in Fig. 7. The two medium-level sphere measurements agreed with each other to within approximately 1% over the entire wavelength range. However, no additional measurements were made to assess the longer term stability and repeatability of the instrument.

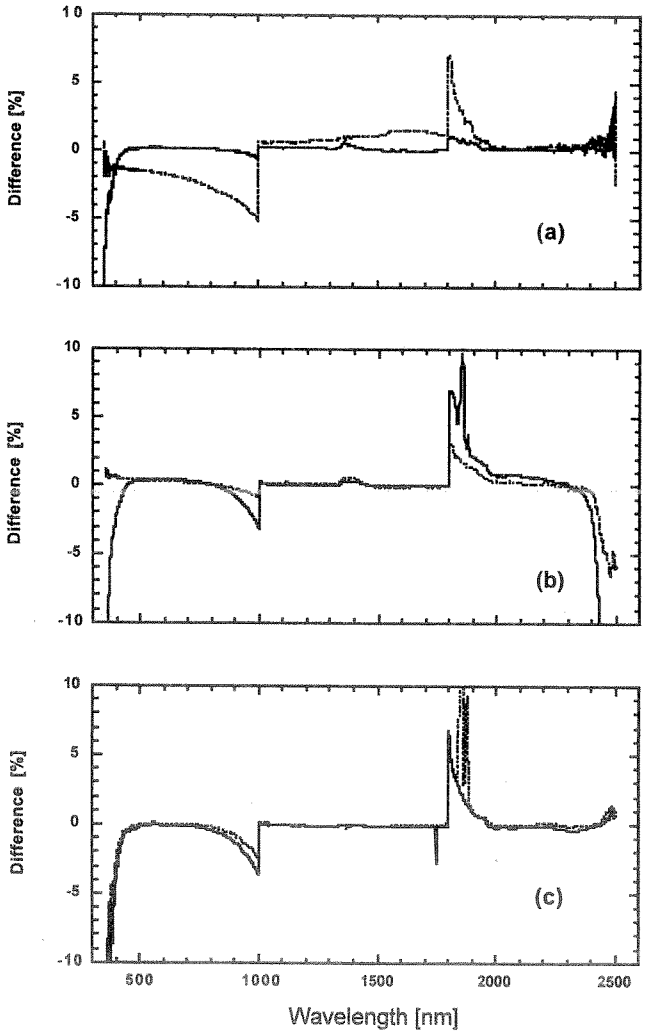

Fig. 6. Difference in (a) the UA, (b) the SDSU, and (c) the JPL FieldSpec FR sphere radiance measurements taken on the 18th of June (dashed line) and the 19th of June (solid line). Measurements were taken approximately 1 h apart for each instrument on each day.

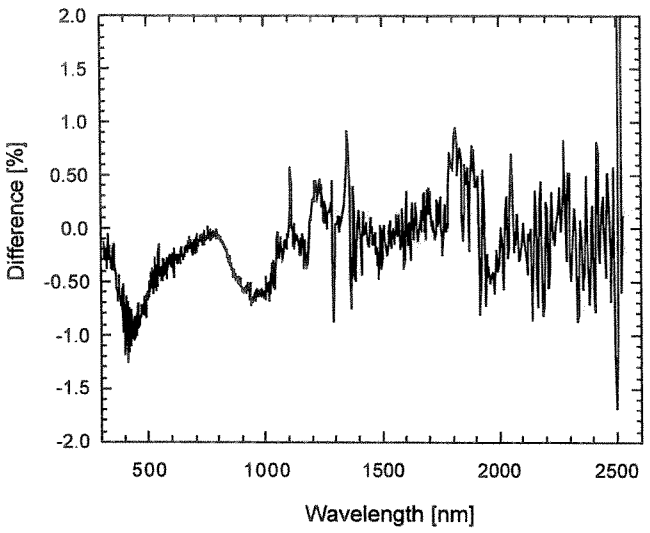

Fig. 7. Difference in sphere radiance measured by the GER Mark V IRIS instrument on the 18th of June. The measurements were made approximately 15 min apart.

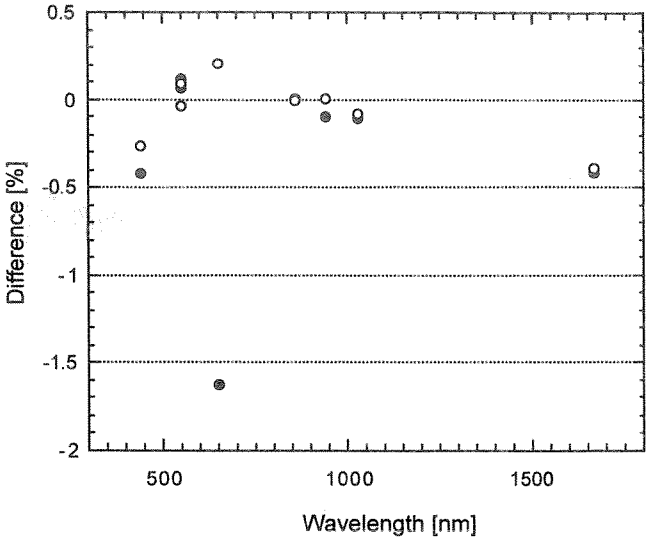

Fig. 9. Difference in sphere radiance measurements taken by the PARABOLA instrument on the 18th of June (open circles) and the 19th of June (closed circles). Measurements on individual days were taken approximately 1 h apart.

Measurements were also made of the medium-level sphere radiance with the GER 3700 instrument after a 3-h warm-up. The measurements were made 1 h apart. As shown in Fig. 8, clear differences are observed for each of the detector regions. The average difference between the two measurements in spectral region where the Si diode array is used is approximately 0.5%, increasing slightly for wavelengths above 800 nm to approximately 1% at 1000 nm. The spectral region using the first PbS detector from 1050 to 1850 nm showed an average offset of approximately 5% in the measured radiance, with a variation about the constant offset of approximately 0.3%. In the spectral region from 1850 to 2500 nm, where the second PbS detector is used, a variability of approximately 0.2% was observed within an average offset of 4%. These differences are attributed to changes in the instrument responsivity arising from variations in the thermal environments of the three array detectors.

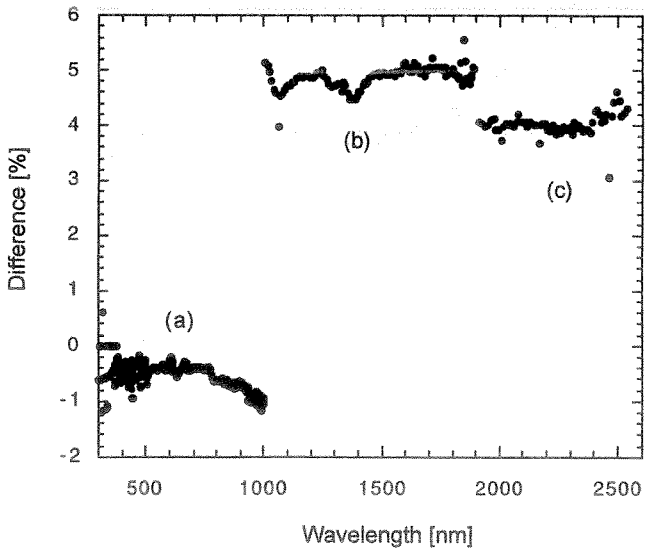

Fig. 8. Difference in sphere radiance measured by the GER 3700. Measurements were made approximately 1 h apart on the 18th of June. A Si array detector was used for region (a), a PbS array detector for region (b), and a second PbS array detector for region (c).

The PARABOLA instrument measured the medium-level sphere radiance twice on both the 18th and the 19th of June. Measurements on each day were separated in time by approximately 1 h. The results are shown in Fig. 9. With the exception of the 650-nm channel, all measurements agreed with each other to within 0.5%. The measurement of the sphere radiance on the 19th of June with the 650-nm channel showed a relative difference of 1.6%. PARABOLA measurements taken on the 18th and 19th of June were also compared and agreed within the combined uncertainties of the measurements taken on the individual days.

4.3. Linearity measurements

To assess the linearity of the instrument response in the visible wavelength region, the sphere radiance at all three lamp levels was measured by two field instruments, the UA FieldSpec FR and the PARABOLA, and compared with the radiance measured by the VXR. The ratios of the medium- to high-level sphere radiance and the low- to high-level sphere radiance for the FieldSpec FR, the PARABOLA, and the VXR are shown in Fig. 10. The ratios of the sphere levels measured by PARABOLA agree with the ratios measured by the VXR to within approximately 6%, and no discernable trend is observed. The ratios of the sphere

levels measured by the UA FieldSpec FR agree with the ratios measured by the VXR to within approximately 4%. In this case, a small offset is observed between the VXR and the UA FieldSpec FR for the ratio of the medium- and high-level sphere radiances. However, it is unclear whether this offset reflects a nonlinearity in the response of the instrument, or is simply due to temporal instabilities in the instrument response.

4.4. Absolute radiance

In certain applications, the field instruments measure the absolute radiance of a source. The SDSU FieldSpec FR was calibrated for spectral radiance less than 1 month before the measurements at the UA. The relative uncertainty of the calibration was approximately 5% over the entire spectral range from 350 to 2500 nm. To verify the accuracy of the calibration and to assess the suitability of the FieldSpec FR instrument for absolute radiance measurements, the medium-level sphere radiance measured by the SDSU FieldSpec FR was compared with the radiance measured by the transfer radiometers.

The second data set taken by the SDSU FieldSpec FR on the 18th of June was used in the evaluation. A cubic spline fit to the data was used to interpolate SDSU FieldSpec FR radiance values to VXR and UA SWIR center wavelengths. Results are shown in Fig. 11. The difference between the sphere radiance measured by the VXR and the SDSU FieldSpec FR varied from 0.25% at 411.53 nm to 5.2% at 774.78 nm. In the infrared region, the difference between the FieldSpec FR and the UA SWIR radiance varied from 8.9% at 1243.5 nm to 16.7% at 2403.2 nm. These results are similar to those obtained for an integrating sphere source, where the calibrated radiance differed from the radiance measured with the transfer radiometers by less than 3% in the visible, and up to approximately 10% in the short-wave infrared (Yoon, Johnson, Kelch, Biggar, & Spyak, 1998).

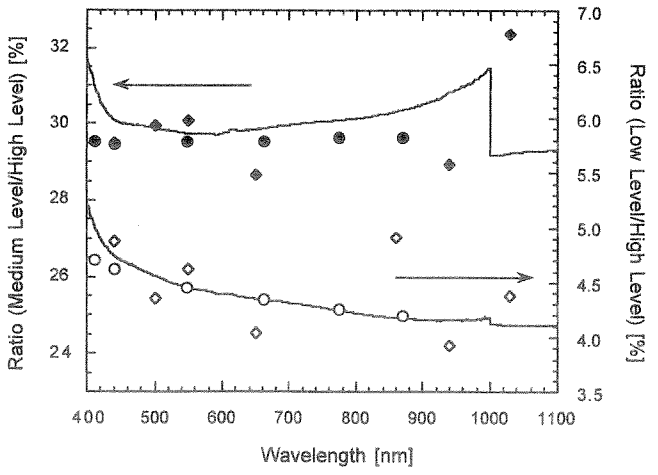

Fig. 10. Ratios of the medium- to high-level sphere radiance (solid symbols) and low- to high-level sphere radiance (open symbols) for the UA FieldSpec FR (solid line), the VXR (circles), and PARABOLA (diamonds).

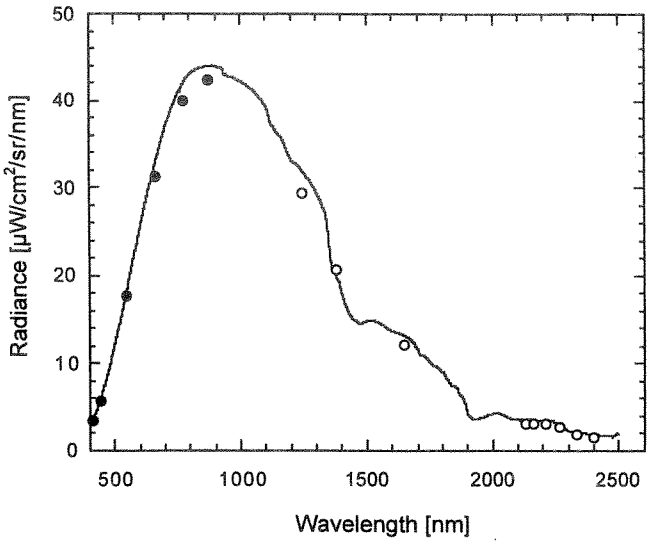

Fig. 11. Absolute radiance measurements of the medium-level sphere radiance with the SDSU FieldSpec FR (solid line), the VXR (closed circles), and the UA SWIR (open circles).

5. Summary

In this experiment, a number of field instruments measured the radiance of a stable integrating sphere source in a controlled laboratory environment to assess their measurement stability. In some cases, instrument performance improved dramatically when the instruments were turned on prior to use (e.g., Fig. 6(a)). However, other instruments continued to show large changes in responsivity after a several-hour warm-up (Fig. 8). These changes in instrument responsivity are largely attributed to thermal variations of the array detectors. Consequently, the detectors should be temperature-stabilized if possible. This is especially critical for field measurements because the detector temperature can change drastically during the course of the measurements as instruments heat up (or cool down) due to environmental conditions.

In addition, further instrument characterization would be useful to fully assess the accuracy of both laboratory and field measurements. For instance, the wavelength accuracy and reproducibility, the stray light rejection, and the out-of-field response of the instruments should be measured, and their effects on measurement uncertainty evaluated. Characterization of the instruments in the field, including measurements of the spectral responsivity, can also aid in developing a more-complete understanding of their operating characteristics (Early et al., 1997; Johnson, Shaw, Hooker, & Lynch, 1998). Knowledge of the instrument performance, along with target measurement wavelengths

and uncertainties can assist in the design of measurement protocols to achieve the required overall measurement accuracy for ground-truth calibrations of satellite sensors.

References

Analytical Spectral Devices, 4760 Walnut Street Suite 105, Boulder, CO 80309, USA.

Biggar, S. F. (1998). Calibration of a visible and near-IR portable transfer radiometer. *Metrologia, 35*, 701–706.

Biggar, S. F., & Slater, P. N. (1993). Preflight cross-calibration radiometer of EOS AM-1 platform visible and near-IR sources. *Proceedings of the International Society of Optic Engineering, 1939*, 243–249.

Deering, D. W., & Leone, P. (1986). Sphere-scanning radiometer for rapid directional measurements of sky and ground radiance. *Remote Sensing of the Environment, 19*, 1–14.

Early, E. A., Thompson, E. A., Johnson, B. C., DeLuisi, J., Disterhoft, P., Wardle, D., Wu, E., Mou, W., Sun, Y., Lucas, T., Mestechkina, T., Harrison, J., Berndt, J., & Hayes, D. S. (1997). The 1995 North American interagency intercomparison of ultraviolet monitoring spectroradiometers. *Journal of Research of the National Institute of Standards and Technology, 103*, 15–62.

Geophysical and Environmental Research Corporation, One Bennett Common, Millbrook, NY 12545.

Johnson, B. C., Fowler, J. B., & Cromer, C. L. (vol. 1–1998). The SeaWiFS Transfer Radiometer (SXR). In: S. B. Hooker, & E. R. Firestone (Eds.), *SeaWiFS postlaunch technical report seriesNASA Technical Memorandum-1998-206892* (pp. 1–58). Greenbelt, MD 20771: NASA Goddard Space Flight Center.

Johnson, B. C., Shaw, P.-S., Hooker, S. B., & Lynch, D. (1998). Radiometric and engineering performance of the SeaWiFS Quality Monitor (SQM): a portable light source for field radiometers. *Journal of Atmospheric and Oceanic Technology, 15*, 1008–1022.

Slater, P. N., Biggar, S. F., Thome, K. J., Gellman, D. I., & Spyak, P. R. (1996). Vicarious radiometric calibrations of EOS sensors. *Journal of Atmospheric and Oceanic Technology, 13*, 349–359.

Thome, K., Schiller, S., Conel, J., Arai, K., & Tsuchida, S. (1998). Results of the 1996 Earth Observing System vicarious calibration joint campaign to Lunar Lake Playa, Nevada (USA). *Metrologia, 35*, 631–638.

Yoon, H., Johnson, B. C., Kelch, D., Biggar, S., & Spyak, P. (1998). A 400 nm to 2500 nm absolute spectral radiance comparison using filter radiometers. *Metrologia, 35*, 563–568.